

## Effect of leaning angle of gecko-inspired slanted polymer nanohairs on dry adhesion

Hoon Eui Jeong, Jin-Kwan Lee, Moon Kyu Kwak, Sang Heup Moon, and Kahp Yang Suh

Citation: *Applied Physics Letters* **96**, 043704 (2010); doi: 10.1063/1.3298554

View online: <http://dx.doi.org/10.1063/1.3298554>

View Table of Contents: <http://scitation.aip.org/content/aip/journal/apl/96/4?ver=pdfcov>

Published by the *AIP Publishing*

---

### Articles you may be interested in

[Prediction of the adhesive behavior of bio-inspired functionally graded materials against rough surfaces](#)

*AIP Advances* **4**, 067143 (2014); 10.1063/1.4886380

[Adhesion tilt-tolerance in bio-inspired mushroom-shaped adhesive microstructure](#)

*Appl. Phys. Lett.* **104**, 011906 (2014); 10.1063/1.4860991

[Effect of pre-tension on the peeling behavior of a bio-inspired nano-film and a hierarchical adhesive structure](#)

*Appl. Phys. Lett.* **101**, 163702 (2012); 10.1063/1.4758481

[Directional adhesion of gecko-inspired angled microfiber arrays](#)

*Appl. Phys. Lett.* **93**, 191910 (2008); 10.1063/1.3006334

[The effect of shape and size in micro-/nanodimples adhesion](#)

*J. Appl. Phys.* **98**, 014310 (2005); 10.1063/1.1944907

---

The advertisement features a dark blue background with a film strip graphic on the left. The text is in white and orange. The main headline reads 'Not all AFMs are created equal' in orange, followed by 'Asylum Research Cypher™ AFMs' in white, and 'There's no other AFM like Cypher' in orange. Below this is the website 'www.AsylumResearch.com/NoOtherAFMLikeIt' in white. In the bottom right corner is the Oxford Instruments logo, which consists of the word 'OXFORD' in a large font above 'INSTRUMENTS' in a smaller font, all within a white rectangular border. Below the logo is the tagline 'The Business of Science®' in a small white font.

## Effect of leaning angle of gecko-inspired slanted polymer nanohairs on dry adhesion

Hoon Eui Jeong,<sup>1</sup> Jin-Kwan Lee,<sup>2</sup> Moon Kyu Kwak,<sup>1</sup> Sang Heup Moon,<sup>2,a)</sup> and Kahp Yang Suh<sup>1,3,b)</sup>

<sup>1</sup>*School of Mechanical and Aerospace Engineering, Seoul National University, Seoul 151-742, Republic of Korea*

<sup>2</sup>*School of Chemical and Biological Engineering, Seoul National University, Seoul 151-742, Republic of Korea*

<sup>3</sup>*World Class University (WCU) Program on Multiscale Mechanical Design, Seoul National University, Seoul 151-742, Republic of Korea*

(Received 20 July 2009; accepted 28 December 2009; published online 29 January 2010)

We present analysis of adhesion properties of angled polymer nanohairs with a wide range of leaning angles from 0° to 45° and ultraviolet (UV)-curable polyurethane acrylate (PUA) materials of two different elastic moduli (19.8 and 320 MPa). It is demonstrated that shear adhesion and adhesion hysteresis can be greatly enhanced by increasing the leaning angle of nanohairs both for soft and hard materials due to increased contact area and reduced structural stiffness. © 2010 American Institute of Physics. [doi:10.1063/1.3298554]

Recent studies have revealed that many structural features such as size, aspect ratio (AR), leaning angle (LA), tip shape, and hierarchy are important to develop an artificial dry adhesive with superior performance.<sup>1</sup> In particular, the directional angle of a hairy surface plays a key role in the anisotropic adhesion property.<sup>2</sup> In addition, the directional angle significantly lowers the effective modulus, resulting in a soft, tacky surface even with a rigid material. Motivated by these fascinating features, a number of methods have been developed to create geckolike high AR, angled structures.<sup>3–8</sup> Despite its significant role in the performance of dry adhesion, however, the effect of LA has not been studied in depth, in part due to technical difficulty in the fabrication of slanted nanohairs with tailored geometry.

In this letter, we fabricate gecko-inspired slanted polymer nanohairs with various LAs and analyze their structural characteristics with particular emphasis on the performance of shear adhesion. For the fabrication, we used a simple two-step method by combining angled etching and replica molding technique as reported earlier.<sup>9</sup> Figures 1(a)–1(d) show scanning electron microscopy (SEM) images of Si master substrates having etched nanoholes with different LAs ( $\varphi_i$ ) of 0°, 15°, 30°, and 45° with respect to the vertical plane. After preparing etched Si masters with angled nanoholes, slanted nanohairs with four different LAs were fabricated by replicating the masters with UV-curable PUA materials of two different Young's moduli as follows: soft (s) PUA (s-PUA, 19.8 MPa) and hard (h) PUA (h-PUA, 320 MPa) [see Figs. 1(e)–1(h)].<sup>10</sup>

To measure the adhesion properties of the slanted nanohairs, the macroscopic shear adhesion strength was evaluated by a hanging test, in which a flexible dry adhesive patch (size: 1 × 1 cm<sup>2</sup>) was attached against a glass surface under a preload of 0.3 N/cm<sup>2</sup>. During the shear adhesion test, no external normal load was applied. Figure 2(a) shows the shear adhesion force of s-PUA nanohairs as a function of

LA. As shown in Fig. 2(a), a significant increase in the shear adhesion was observed with the increase of LA. The shear adhesion of vertical nanohairs was ~9.3 N/cm<sup>2</sup>, which was enhanced to ~18.9 N/cm<sup>2</sup> with LA of 15°. The shear adhesion with 30° and 45° were further increased to ~28.5 and 38.1 N/cm<sup>2</sup>, respectively, suggesting that the shear adhesion increases with increasing LA. One notable feature is that the shear adhesion force of s-PUA nanohairs (20–40 N/cm<sup>2</sup>) was greatly increased as compared to that of h-PUA nanohairs [5–15 N/cm<sup>2</sup>, see Fig. 3(a)]. This can be attributed to two reasons. The first is the higher surface energy of s-PUA (~40 mJ/m<sup>2</sup>) compared to that of h-PUA (~30 mJ/m<sup>2</sup>), resulting in the higher work of adhesion. The second is the side contact caused by the reduced structural stiffness. Since the elastic modulus of s-PUA (~19.8 MPa) is an order of magnitude lower than that of h-PUA (~320 MPa), the bending would be much higher accordingly, resulting in side contact rather than tip contact.

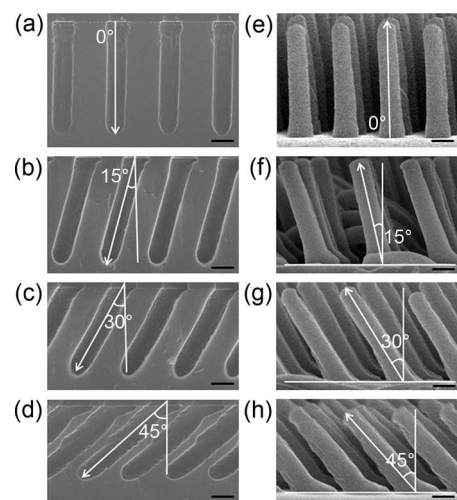


FIG. 1. [(a)–(d)] SEM images of the Si master substrates having angled etch profiles with LAs of 0°, 15°, 30°, and 45°, respectively. [(e)–(h)] SEM images of the h-PUA nanohairs (2 μm length and 400 nm diameter) replicated from the masters shown in (a)–(d). (Scale bar=400 nm.)

<sup>a)</sup> Author to whom correspondence should be addressed. Electronic mail: shmoon@surf.snu.ac.kr.

<sup>b)</sup> Electronic mail: sky4u@snu.ac.kr.

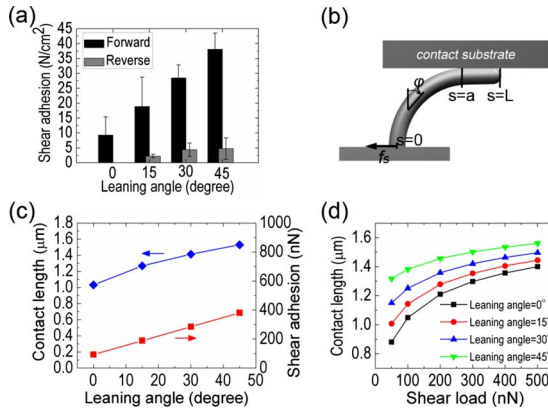


FIG. 2. (Color online) (a) Measurement of macroscopic shear adhesion force with an adhesive patch (thickness: 50–60  $\mu\text{m}$ ,  $D=1.0\times 10^8/\text{cm}^2$ , and size:  $1\times 1\text{ cm}^2$ ) having s-PUA nanohairs with different LAs against smooth glass surface after removing preload of 0.3  $\text{N}/\text{cm}^2$ . (b) A schematic drawing of the deflected s-PUA nanohair under a shear load of  $f_s$ . (c) Theoretical side contact lengths (blue diamond) of s-PUA nanohair along with experimental shear adhesion force of single s-PUA nanohair (red box). (d) Theoretical side contact lengths of s-PUA nanohairs with four different LAs as a function of applied shear load.

The maximum shear adhesion force of single nanohair can be written by<sup>11,12</sup>

$$F_S = A \times \tau = L_C \times W_C \times \tau, \quad (1)$$

where  $A$  is the contact area,  $\tau$  is the interfacial shear strength,  $L_C$  is the side contact length, and  $W_C$  is the contact width. Here  $W_C$  can be expressed as<sup>12</sup>

$$W_C = 8 \left\{ \frac{(1-\nu^2)R^2W_{12}}{\pi E} \right\}^{1/3}, \quad (2)$$

where  $\nu$  is the Poisson's ratio,  $R$  is the radius,  $E$  is the elastic modulus of nanohair, and  $W_{12}$  is the work of adhesion between nanohair and contact substrate. For the s-PUA nanohair, the contact width is expected to be  $\sim 215\text{ nm}$  from Eq. (2). By considering a single s-PUA nanohair as an elastic rod, the side contact length ( $L_C=L-a$ ) for a given shear load ( $f_s$ ) acting on the tip of the nanohair can be obtained by solving the ordinary differential equation [see Fig. 2(b)]<sup>13,14</sup>

$$\varphi'' + \frac{f_s}{EI} \cos \varphi = 0, \quad (3)$$

where  $I$  is the moment of inertia of nanohair and the corresponding boundary conditions are as follows:<sup>13,14</sup>

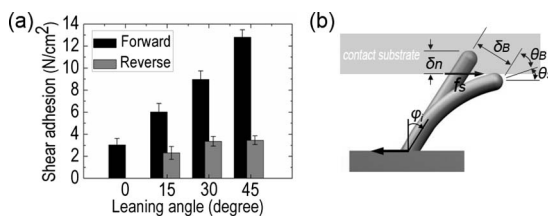


FIG. 3. (a) Measurement of macroscopic shear adhesion force with an adhesive patch (thickness: 50–60  $\mu\text{m}$ ,  $D=1.0\times 10^8/\text{cm}^2$ , and size:  $1\times 1\text{ cm}^2$ ) having h-PUA nanohairs with different LAs against smooth glass surface after removing preload of 0.3  $\text{N}/\text{cm}^2$ . (b) A schematic drawing of the deflected h-PUA nanohair under a shear load of  $f_s$ .

$$\varphi(0) = \varphi_i, \quad \varphi(a) = \frac{\pi}{2}, \quad \varphi'(a) = \sqrt{\frac{2w}{EI}}. \quad (4)$$

Here,  $w$ , the adhesion energy per length, is given by<sup>12</sup>

$$w = 6 \left\{ \frac{(1-\nu^2)R^2W_{12}^4}{\pi E} \right\}^{1/3}. \quad (5)$$

Figure 2(c) shows the theoretical predictions of the contact length ( $L_C=L-a$ ) by solving the above boundary value problem, along with the measured shear adhesion ( $f_s$ ) of single s-PUA nanohair as a function of LA. Interestingly, the side contact length of the s-PUA nanohair was over  $1\text{ }\mu\text{m}$  and gradually increased with the increase of LA. The contact length of vertical nanohair was  $\sim 1.0\text{ }\mu\text{m}$ , which was enhanced to  $\sim 1.3\text{ }\mu\text{m}$  with LA of  $15^\circ$ . The contact length with  $30^\circ$  and  $45^\circ$  were further increased to  $\sim 1.4$  and  $1.5\text{ }\mu\text{m}$ , respectively, suggesting that the s-PUA nanohairs make a strong side contact with the substrate and the contact length increases with increasing LA. For the theoretical predictions in Fig. 2(c), the applied shear load ( $f_s$ ) was estimated to be  $\sim 93\text{ nN}$  ( $\varphi_i=0^\circ$ ),  $189\text{ nN}$  ( $\varphi_i=15^\circ$ ),  $285\text{ nN}$  ( $\varphi_i=30^\circ$ ), and  $381\text{ nN}$  ( $\varphi_i=45^\circ$ ) from the experimental results [Fig. 2(a)], assuming all hairs ( $1.0\times 10^8/\text{cm}^2$ ) are in contact with the substrate. By assuming the interfacial shear strength as  $\sim 7\text{ MPa}$ ,<sup>11</sup> the predicted shear adhesion forces are  $\sim 1.5$ ,  $1.9$ ,  $2.1$ , and  $2.3\text{ }\mu\text{N}$  for nanohairs with LAs of  $0^\circ$ ,  $15^\circ$ ,  $30^\circ$ , and  $45^\circ$ , respectively. These values are about an order of magnitude higher than the experimental results. This discrepancy can be attributed to several reasons such as inaccurate estimate of  $\tau$ , surface roughness of nanohairs, mating of nanohairs, water layers formed on solid surfaces, contact fracture due to elongation of soft nanohairs or backing membrane buckling.<sup>13</sup> Nonetheless, it is obvious that the side contact length is gradually enhanced with the increase in LA of s-PUA nanohairs as shown in Fig. 2(c). To see whether the side contact length is affected by LA under the same shear load, we estimated the contact length of nanohairs with four different LAs as a function of applied shear load ( $f_s$ ). As shown in Fig. 2(d), even under the same shear load, the side contact length increases with the increase of LA. Furthermore, the nanohairs with a higher LA can have a higher contact length even under a low shear load, demonstrating the reduced structural stiffness of slanted nanohair.

As the bending and rotation of nanostructures strongly depend on mechanical properties of materials used,<sup>15</sup> we also fabricated the same nanohairs with h-PUA ( $E\sim 320\text{ MPa}$ ) and examined their adhesion properties. According to Eq. (3), the h-PUA nanohairs are expected to make a tip contact with the substrate rather than a side contact since the elastic restoring force is larger than surface forces for adhesion due to high elastic modulus and relatively low work of adhesion.<sup>12,14</sup> As a result, it is expected that the variation in shear adhesion of h-PUA nanohairs would be small with different LAs. Our experimental results, however, showed that the shear adhesion forces are still increased with the increase in LA [Fig. 3(a)]. This means that although the h-PUA nanohairs would be difficult to form a side contact with the substrate, the actual contact area around the tip of nanohairs is increased by increasing the structural LAs when a shear load is applied. This can be explained in terms of the reduced structural stiffness as follows: When a shear force ( $f_s$ ) is

applied to a tilted cantilever, the normal deflection ( $\delta_n$ ) and the rotation angle ( $\theta_B$ ) are given by [see Fig. 3(b)]<sup>15,16</sup>

$$\delta_n = \frac{L^3 f_S \sin \varphi_i \cos \varphi_i}{3EI}, \quad \theta_B = \frac{L^2 f_S \cos \varphi_i}{2EI}, \quad (6)$$

where  $L$  is the hair length. Assuming all hairs ( $1.0 \times 10^8/\text{cm}^2$ ) are in contact with the substrate,  $f_S$  is estimated to be  $\sim 30$  nN ( $\varphi_i=0^\circ$ ), 60 nN ( $\varphi_i=15^\circ$ ), 90 nN ( $\varphi_i=30^\circ$ ), and 130 nN ( $\varphi_i=45^\circ$ ) from the experimental results. Under these shear loads, the values of  $\delta_n$  are  $\sim 0$  nm ( $\varphi_i=0^\circ$ ), 100 nm ( $\varphi_i=15^\circ$ ), 260 nm ( $\varphi_i=30^\circ$ ), and 430 nm ( $\varphi_i=45^\circ$ ), and the values of bending angle ( $\theta_s \approx 90^\circ - \varphi_i - \theta_B$ ) are reduced to  $\sim 81^\circ$ ,  $58^\circ$ ,  $38^\circ$ , and  $19^\circ$  from their initial angles of  $90^\circ$ ,  $75^\circ$ ,  $60^\circ$ , and  $45^\circ$ , respectively. This suggests that nanohairs with higher LAs are more compliant<sup>15,16</sup> and can make more intimate contact with the substrate, resulting in an enhanced adhesion. However, there is a trade-off in the adhesion performance for a higher LA in that the adaptability to a rough surface would become lower.<sup>9</sup> In addition, slanted nanohairs with higher LA are prone to clumping on the substrate.<sup>6</sup> It is noted in this regard that the gecko overcomes this limitation through hierarchically organized multiscale hairs.<sup>9,17</sup>

In summary, our experimental and theoretical studies have demonstrated that shear adhesion and adhesion hysteresis can be greatly increased by enhancing the LA of nanohairs both for soft and hard materials due to increased contact area and reduced structural stiffness.

This work was supported by the Nano R&D Program (Grant No. 2007-02605), the Center for Nanoscale Mecha-

tronics & Manufacturing (Grant No. 08K1401-00210), and King Abdullah University of Science and Technology (KAUST) program (Grant No. KUK-F1-037-02). This work was also supported in part by the Center for Ultramicrochemical Process Systems.

<sup>1</sup>H. E. Jeong and K. Y. Suh, *Nanotoday* **4**, 335 (2009).

<sup>2</sup>B. X. Zhao, N. Pesika, H. B. Zeng, Z. S. Wei, Y. F. Chen, K. Autumn, K. Turner, and J. Israelachvili, *J. Phys. Chem. B* **113**, 3615 (2009).

<sup>3</sup>B. Aksak, M. P. Murphy, and M. Sitti, *Langmuir* **23**, 3322 (2007).

<sup>4</sup>M. P. Murphy, B. Aksak, and M. Sitti, *Small* **5**, 170 (2009).

<sup>5</sup>S. Reddy, E. Arzt, and A. del Campo, *Adv. Mater.* **19**, 3833 (2007).

<sup>6</sup>T. Kim, H. E. Jeong, K. Y. Suh, and H. H. Lee, *Adv. Mater.* **21**, 2276 (2009).

<sup>7</sup>S. Kim, M. Spenko, S. Trujillo, B. Heyneman, D. Santos, and M. R. Cutkosky, *IEEE Trans. Robot.* **24**, 65 (2008).

<sup>8</sup>J. H. Lee, R. S. Fearing, and K. Komvopoulos, *Appl. Phys. Lett.* **93**, 191910 (2008).

<sup>9</sup>H. E. Jeong, J. K. Lee, H. N. Kim, S. H. Moon, and K. Y. Suh, *Proc. Natl. Acad. Sci. U.S.A.* **106**, 5639 (2009).

<sup>10</sup>P. J. Yoo, S. J. Choi, J. H. Kim, D. Suh, S. J. Baek, T. W. Kim, and H. H. Lee, *Chem. Mater.* **16**, 5000 (2004).

<sup>11</sup>C. M. Pooley and D. Tabor, *Proc. R. Soc. London, Ser. A* **329**, 251 (1972).

<sup>12</sup>C. S. Majidi, R. E. Groff, and R. S. Fearing, *J. Appl. Phys.* **98**, 103521 (2005).

<sup>13</sup>J. H. Lee, C. S. Majidi, B. Schubert, and R. S. Fearing, *J. R. Soc., Interface* **5**, 835 (2008).

<sup>14</sup>C. S. Majidi, *Mech. Res. Commun.* **36**, 369 (2009).

<sup>15</sup>J. M. Gere and S. P. Timoshenko, *Mechanics of Materials*, 4th ed. (PWS, Boston, 1997).

<sup>16</sup>K. Autumn, C. Majidi, R. E. Groff, A. Dittmore, and R. Fearing, *J. Exp. Biol.* **209**, 3558 (2006).

<sup>17</sup>K. Autumn, Y. A. Liang, S. T. Hsieh, W. Zesch, W. P. Chan, T. W. Kenny, R. Fearing, and R. J. Full, *Nature (London)* **405**, 681 (2000).